JOURNAL OF Applied Polymer SCIENCE

Geometrical Bowing and Molecular Orientation Angle in Biaxially Stretched Poly(ethylene terephthalate) Films

Alois Koerber,[1] Roland Lund,[1] Horst-Christian Langowski[2,3]

[1]Brueckner Maschinenbau GmbH & Co. KG, Koenigsberger Str. 5-7, 83313 Siegsdorf, Germany

[2]TU Muenchen, Weihenstephaner Steig 22, 85350 Freising, Germany

[3]Fraunhofer IVV, Giggenhauser Str. 35, 85354 Freising, Germany

Correspondence to: A. Koerber (E-mail: alois.koerber@brueckner.de)

ABSTRACT: The aim of this study was to investigate in greater detail the occurrence of geometrical bowing and the average molecular orientation direction in biaxially stretched and annealed film webs and to determine possible causes for these effects at a morphological level. This involved studying the temperature-dependent behavior of annealed and nonannealed film webs and determining the geometrical bowing and average molecular orientation direction across the working width of the film. The average molecular orientation direction was measured offline using a polarimeter and also online using a novel online orientation sensor. It was shown that the geometrical bowing correlates directly with the amount of film shrinkage in machine direction which occurs during annealing in the transverse direction orienter. In addition, a possible explanation is given for the greater increase in the molecular orientation angle at the film edges compared with the geometrical bowing. Good agreement was found between online and offline measurement of the molecular orientation angle. © 2012 Wiley Periodicals, Inc. J. Appl. Polym. Sci. 000: 000–000, 2012

KEYWORDS: poly(ethylene terephthalate); biaxial stretching; geometrical bowing; molecular orientation angle

Received 9 November 2011; accepted 20 April 2012; published online
DOI: 10.1002/app.37967

INTRODUCTION

Biaxially stretched films made of poly(ethylene terephthalate) (PET) have high mechanical strength, good insulation and barrier properties, and high dimensional stability when exposed to heat. These materials therefore have a wide range of applications, for example for odor-tight packaging, films for electrical insulation, substrate films for magnetic tapes, and films for photographic and X-ray images. PET films have also been used for some time as optical films in liquid crystal displays and as release films for protecting polarization films during their manufacture and quality testing. For optical applications, the dimensional stability when exposed to heat and the optical quality of the films are foremost. With regard to the latter, freedom from particles and scratches and the polarization characteristics are important.

A detailed description of the process for continuous sequential biaxial stretching of PET films has been published by Heffelfinger[1] and a brief summary of this is worthwhile here. The homogenized polymer melt is extruded through a die onto a chill roll and stretched to suppress the crystallization. The cast film has a volumetric crystallinity value ranging from 0% to about 2.5% depending on the film thickness and rate of cooling. The essentially amorphous cast film is removed from the chill roll, heated to a temperature of about 85°C, and stretched in the longitudinal direction (machine direction, MD). The longitudinal stretching is carried out on stretching rollers having increasing peripheral speeds. The stretching ratio, the temperature of the film in the stretching gap, its length and the rate of stretching largely determine the state of orientation and the morphology of uniaxially stretched films. Stress-induced crystallization starts above a stretching ratio of about 2.3, depending on the stretching temperature and rate of stretching. The volumetric crystallinity can be up to 20% in the uniaxially stretched film. The *c*-axis of the fibrillar crystallite structures is mostly in the stretching direction, and the benzene ring planes orientate themselves increasingly parallel to the film surface with increasing orientation.

After longitudinal stretching, the film is stretched in the transverse direction orienter (TDO) in the transverse direction (TD), perpendicular to the MD. Some of the fibrillar crystallites change orientation from the MD to the TD.[2] At the end of the transverse stretching the crystalline and noncrystalline regions

are preferentially orientated in the direction of the second stretching and the amount of stress-induced crystallinity has increased by about 5%. To dissipate internal stress and to facilitate thermal stabilization, the film is annealed in the TDO at fixed dimensions after the transverse stretching. The heating to temperatures just below the melting temperature of the polymer results in melting of existing crystallite fibrils. In addition, amorphous molecular chains that are under stress relax and subsequently settle on existing crystalline regions. The volumetric crystallinity of the film increases during annealing by 20–25% and thus reaches about 45–50% in the final biaxially stretched and annealed film.

Chang et al.[3] analyzed the morphology of sequentially biaxially stretched films. Studies on films stretched on a laboratory stretching frame showed that immediately after the second stretching there are two crystallite populations in the film whose *c*-axis is orientated in the direction of the first and second stretching. For transverse stretching ratios equal to or greater than the longitudinal stretching ratio, both the crystalline and amorphous regions in the stretched film are primarily orientated in the direction of the second stretching—and hence also the average orientation as a sum of the amorphous and crystalline orientation. Although the MD average orientation decreases again with increasing TD stretching ratio, it is considerably higher in the biaxially stretched film compared with the cast film. The fibrillar crystallite structures in the MD and TD that are present after the second stretching act as crystallization nuclei for thermal crystallization during annealing. In this phase, there is conversion of the MD and TD fibrils into lamellar structures, existing crystallites melt and grow primarily perpendicular to the existing *c*-axis orientation and in the thickness direction.

Gohil[4] also describes the sequence of the reorientation of the amorphous and crystalline regions during the second stretching for films that had been sequentially biaxially stretched on a laboratory stretching frame. It was found that with increasing transverse stretching there was first a reorientation of the crystalline regions and isotropic crystalline orientation in the film plane. On further increase of the TD stretching ratio, there is then isotropic average orientation—the overall orientation of the crystalline and amorphous regions—before finally the amorphous regions also attain an isotropic orientation state. Before reaching a balanced MD/TD stretching ratio, both the crystalline and amorphous regions in the film plane are largely orientated in the direction of the second stretching. It was also observed that isotropic crystalline orientation causes isotropic shrinkage, that isotropic amorphous orientation leads to isotropic properties such as tensile strength and elongation at break and that isotropic average orientation leads to isotropic E-modulus values.[4]

In general, the chains of the macromolecules strive to attain a fully relaxed state, corresponding to the state of maximum entropy. The entropy falls during the stretching with increasing orientation of the molecular chains. This striving of the orientated molecular chains to return to the state of maximum entropy results in a relaxation force in the orientated polymer.[5,6]

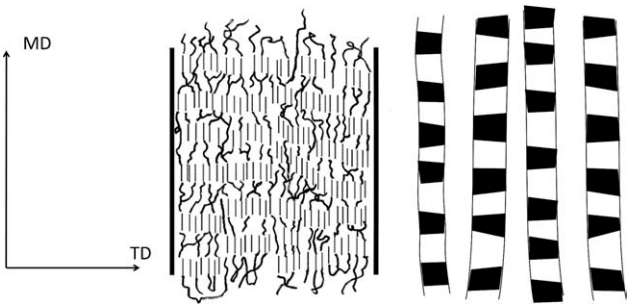

Figure 1. Schematic representation of uniaxially stretched PET in accordance with Cakmak (left)[11] and Gohil (right).[3]

The desire of metastable MD-orientated *trans* molecules in the amorphous regions to change to *gauche* conformation via chain relaxation is termed to be the main reason for thermal shrinkage in thermoplastics at temperatures above the glass transition temperature.[2,7,8]

Prevorsek et al.[9] proposed a model for orientated fibers whereby the overall shrinkage was based on the relaxation of two different amorphous regions. The intrafibrillar amorphous regions connect adjacent crystallites within the microfibrils. Their relaxation represents the preferred mechanism for low degrees of contraction, while at high degrees of contraction the relaxation of the interfibrillar tie-molecules in the amorphous regions and the displacement of fibrils dominate.

The presence of different isomers in the amorphous regions in the form of *trans* and *gauche* conformations and their specific absorption bands in the infrared wavelength region has been observed by, among others, Schmidt.[10]

Unwound, orientated chains in the amorphous regions are called *trans* isomers, while chains in the *gauche* conformation are in the relaxed state and have no defined preferred orientation. In the cast film more than 80% of the molecular chains are in the *gauche* conformation.[7] The number of *trans* isomers increases due to the unwinding of the molecular chains during the first stretching step. With the onset of stress-induced crystallization, a portion of the *trans* isomers in the amorphous regions transforms to the crystalline fibril structure, namely the most energetically favorable state. The stress-induced crystallites act as immobile blocks in an amorphous matrix consisting of molecules with *trans* and *gauche* conformations, causing suppression of a portion of the thermal shrinkage.[5]

Figure 1 shows two possible schematic representations of the structure of a uniaxially stretched PET film. The crystallites that act as network nodes[5] hinder the relaxation of some of the *trans* molecular chains that lie in-between and so partly hinder the shrinkage. During the second stretching step some of the MD crystallites reorientate, while a further portion fracture and the molecular chains align primarily in the TD. This produces an additional TD population of stress-induced crystallites.

Fischer[12] established that the density of both the amorphous and crystalline regions depends on the parameters used for the stretching and annealing. Here, the density of the amorphous regions can approach the density of the crystalline regions

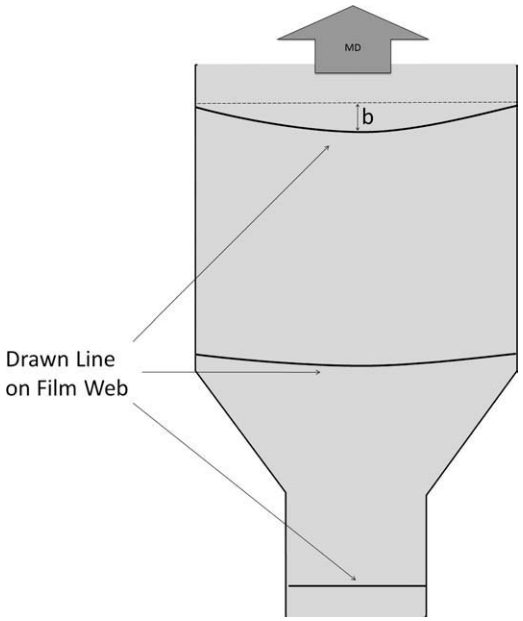

Figure 2. Development of geometrical bowing B during transverse stretching and annealing of a film web.

depending on the degree of orientation of the amorphous *trans* molecular chains due to the stretching. As such, the two phase model is only a very simplified representation of the morphological structure of orientated semicrystalline PET.

One effect which occurs only during stretching of films in the continuous stretching process is called geometrical bowing (Figure 2). A straight line is drawn across the width of a film before the transverse stretching step. During transverse stretching and annealing of the film the straight line changes into a bow. The value *B* of the geometrical bowing of a film web is defined as the maximum deviation of the bow shaped line from a straight line across the film web at the end of the TDO. Films with high geometrical bowing have poor flatness and winding properties and changing property anisotropies across the working width. It is therefore essential to suppress the geometrical bowing as far as possible by taking measures during processing. Yamada[13,14] studied the occurrence of geometrical bowing during sequential biaxial stretching of PET as a function of the processing parameters and identified ways of reducing the bowing by introducing a buffer zone between the transverse stretching zone and annealing zone of the TDO.

MacDonald et al.[15] constitute the development of geometrical bowing to MD stress that is caused by a Poisson ratio effect during TD stretching and subsequent annealing. Because the modulus of the film in the annealing zone is lower than the modulus of the film in the stretching zone the generated MD stress causes a retardation of the center part of the film web compared with its edges. The development of geometrical bowing during TD stretching due to the Poisson ratio effect may be reduced by introducing a low temperature buffer zone between the stretching and the annealing zones of a TDO.[14]

The relaxation of MD oriented *trans* molecules causes MD shrinkage during heating up the biaxially stretched film web from stretching temperature to annealing temperature. At the center part of the film web where the gripping force of the sidewise arranged clips is at its minimum the MD shrinkage causes a maximum geometrical deformation. Because of a decrease in modulus during heating up the film the geometrical deformation due to MD shrinkage causes a retardation of the center part of the film web compared with its edges.

A further aspect of the bowing phenomenon, which solely occurs in continuous stretching plants, is the changing of the average molecule orientation direction across the working width. Yamada[13,14,16] called this phenomenon "characteristical" bowing and studied this for, among other things, sequentially biaxially stretched PET. The angle between the TD and average orientation direction will henceforth here be referred to as the molecular orientation angle.

Jungnickel[17] observed that the principal orientation direction of a biaxially stretched PET film changes across the working width. Using both birefringence and X-ray measurement techniques Jungnickel concluded that the principal orientation direction of both the amorphous and crystalline phase may not coincide outside the center part of the film web. The highest degree of planarity for the benzene ring planes was found to be at the center part of the film web. It was also seen that planarity is significantly decreasing toward the edges. Whereas Jungnickel observed just one preferred crystallite orientation direction, MacDonald et al.[18] detected a second, weaker developed crystallite orientation direction, which was oriented at 90° with respect to the first crystalline orientation direction at the center part of the film web.

Investigations conducted by Kim et al.[19] using a combination of X-ray, fluorescence and refractive index measurements support the conclusion that the orientation directions of the amorphous and the crystalline domains in a sequentially biaxially stretched film web do not coincide across the working width but vary in a different range.

Due to the direct relationship between the average orientation and the refractive indices[20] in the film plane, the direction of the largest and smallest refractive indices also changes across the working width with the molecular orientation angle. The principal refractive indices in the film plane represent the main axes of the index ellipsoid (see Figure 3).

The direction of the largest refractive index in the film plane is termed the slow axis according to the slowest propagation speed

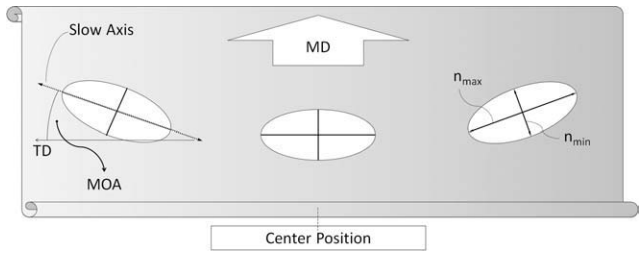

Figure 3. Refractive index ellipsoid with anisotropic refractive indices (n_{max} and n_{min}) and molecular orientation angle in a biaxially stretched film web.

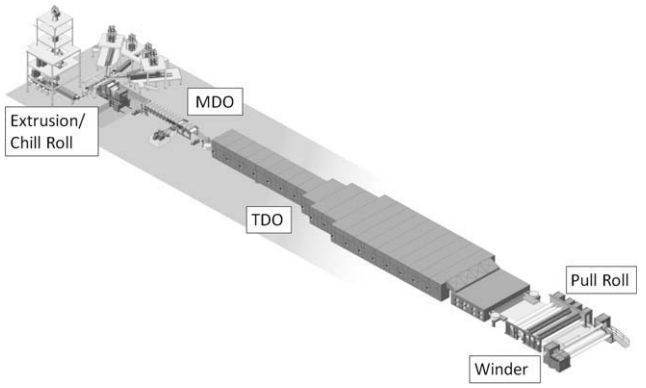

Figure 4. Sequential biaxial film stretching plant (© by Brückner).

of light waves whose electrical field vector oscillates parallel to this direction.

In addition, Blumentritt[2] showed that the average molecular orientation of PET films correlates with the anisotropy of macroscopic film properties. The maximum and minimum of the E-modulus was measured in the direction of the largest and smallest refractive index in the film plane, respectively.

Both geometrical bowing and the anisotropy of the average molecular orientation have been the topic of many studies. Notwithstanding this, there is still a lack of detailed knowledge about the differences and relationships between geometrical bowing and the anisotropy of the average molecular orientation and their dependence on individual process parameters.

The study being reported here investigates the causes of geometrical bowing and the change in the average molecular orientation across the working width in sequentially biaxially stretched PET films. Furthermore, qualitative and quantitative relationships were identified between geometrical bowing, shrinkage in the MD and the average molecular orientation direction. Online measurement of the average molecular orientation direction is described and the results are compared with laboratory measurements.

EXPERIMENTAL

Materials, Equipment, and Stretching Parameters

Sequentially biaxially stretched film rolls were manufactured on the pilot scale stretching unit in the Technology Centre of Brueckner Maschinenbau GmbH & Co. KG. The pilot scale stretching unit is schematically shown in Figure 4. The temperature in the annealing zone of the TDO was the process parameter that was varied (see Table I). A total of 10 film samples that differed in annealing temperature and shrinking temperature were taken and analyzed.

Using a multilayer die a 3-layer film (raw material: Invista RT 4027, average molecular weight M_w = 45,000 g/mol) of ABA structure with 10% antiblocking master batch in the surface layers was extruded and chilled on a chill roll. The glass transition temperature of the cast film was measured using differential scanning calorimetry and found to be 73.8°C. The chilled cast film was heated up to stretching temperature in the MD orienter, stretched by a factor of 3 in the longitudinal direction between rollers having increasing peripheral speeds and cooled. Thereafter the film was passed into the TDO and was heated again to stretching temperature in the preheating zone. The previously uniaxially stretched film was stretched by a factor of 3.4 in the stretching zone of the TDO perpendicular to the MD. The film was then annealed in the annealing zone of the TDO at the temperatures indicated in Table I. Film samples 1–5 were annealed at 70°C. As no relaxation or reorientation processes and no thermal crystallization occur at temperatures below the glass transition temperature in the biaxially stretched film due to the limited mobility of the molecular chains, Film samples 1–5 were used as reference films for nonannealed films which represent the state of the film structure immediately after the stretching. Five more film samples (Samples 6–10) were annealed in the TDO at temperatures between 120°C and 240°C (see Table I). The residence time of the films in the annealing zone of the TDO was about 20 s. After leaving the TDO, the edge of the film was removed and the film was then wound.

The film thickness after the biaxial stretching was 80 μm (final film thickness) and the net width of the film after removing the edge was 800 mm.

Geometrical Bowing

To measure the geometrical bowing, a line across the film web was printed on the upper side of the film web of Film sample rolls 6–10. This was carried out using a print roll before the TDO. After the TDO, the line deviated from the line joining the line positions on the outer edge of the net working width. The deviation $D(x)$ of the line was measured across the working width at 39 points at intervals of 20 mm with an accuracy of ±0.25 mm. The value of the geometrical bowing B is given by

$$B = \left(\frac{B_{\max}}{w}\right)$$

where B, geometrical bowing; $B_{\max}$, measured maximum deviation; and w, net working width.

Table I. MD Shrinkage in Sequentially Biaxially Stretched PET Film Samples Annealed at Different Temperatures in the TDO; Variation of the Free Shrinkage Temperature Between 120 and 240°C

Film sample	TDO annealing temperature (°C)	Free shrinkage temperature (°C)	MD shrinkage (%)
Film sample 1	70	120	18.9
Film sample 2	70	150	20.3
Film sample 3	70	180	23.7
Film sample 4	70	210	28.2
Film sample 5	70	240	35.5
Film sample 6	120	120	14.4
Film sample 7	150	150	14.9
Film sample 8	180	180	15.6
Film sample 9	210	210	16.6
Film sample 10	240	240	16.5

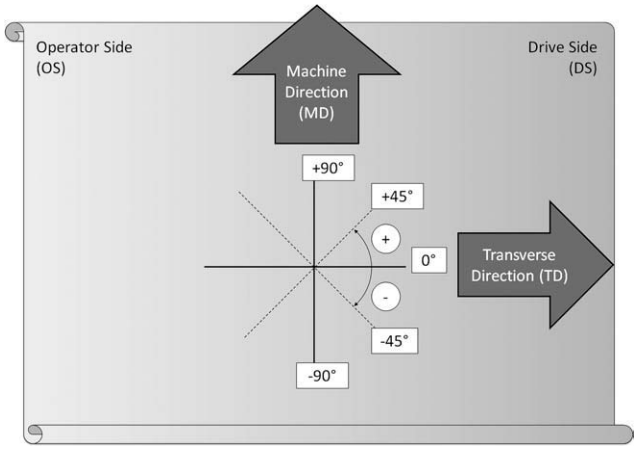

Figure 5. Coordinate system of the Mueller matrix polarimeter (AxoScan) used for offline measurement of the molecular orientation angle (top view of a biaxially stretched film web).

The observed deviation across the working width had an approximately quadratic profile and so the geometrical bowing can be described as follows:

$$D(x) = a \cdot x^2,$$

where

$$a = \left(\frac{B_{\max}}{w^2/4}\right)$$

and $D(x)$, geometrical bowing at position x and x, distance to the center position.

The angle between the geometrical bowing line at position x and the TD of the film web is given by:

$$\beta = \arctan\left(\frac{d(D(x))}{dx}\right)$$

$$\frac{d(D(x))}{dx} = 2ax$$

and β, angle between the geometrical bowing line and the TD of the film web.

Shrinkage

Square film samples (side length 100 mm) were taken from the center of the film webs. These samples were annealed for 30 min in a shrinking oven. Film samples 1–5 (annealed in the TDO at 70°C) were shrunk at temperatures of 120, 150, 180, 210, and 240°C, respectively, for 30 min. The rest of the film samples (Film samples 6–10, annealing temperatures in the TDO of between 120°C and 240°C) were each annealed in the shrinking oven at the identical temperature at which the films had been annealed in the TDO during their manufacture.

The aim of the shrinking tests was to determine the reduction in the MD shrinkage as a result of annealing the films in the TDO of the film production plant and to determine what fraction of the free MD shrinkage is still observed after annealing in the TDO. By measuring the size of the free film samples before and after annealing in the shrinking oven, the shrinkage parallel to the MD (MD shrinkage) was determined.

Offline Measurement of the Molecular Orientation Angle

The films were analyzed in the laboratory to determine the profile of the molecular orientation angle across the working width. The molecular orientation angle was measured offline using a Mueller matrix polarimeter (*AxoScan*™) manufactured by Axometrics. The complete dual rotating retarder polarimeter and the mathematical procedure for deriving the Mueller matrix have been described elsewhere.[21]

The molecular orientation angle was measured with an accuracy of ±0.5°. The coordinate system shown in Figure 5 was used for representing the molecular orientation angle across the working width. Positive angles are shown in a counter-clockwise direction. A molecular orientation angle of 0° corresponds to an average orientation angle perpendicular to the MD.

Online Measurement of the Molecular Orientation Angle

Online measurement of the molecular orientation angle was carried out during the production of Film sample 9 using an online orientation sensor (Figure 6, manufactured by MTD GmbH, Uffing am Staffelsee, Germany). For this purpose, the sensor was mounted such that it could be moved between the TDO and winder on the traverse to which the unit for measuring the final film thickness was also attached.

The online orientation sensor consists of a transmitter module and a receiver module. The transmitter module, which is fixed above the traveling film web, emits monochromatic, circularly

Figure 6. Online measuring system; machine direction from left to right.

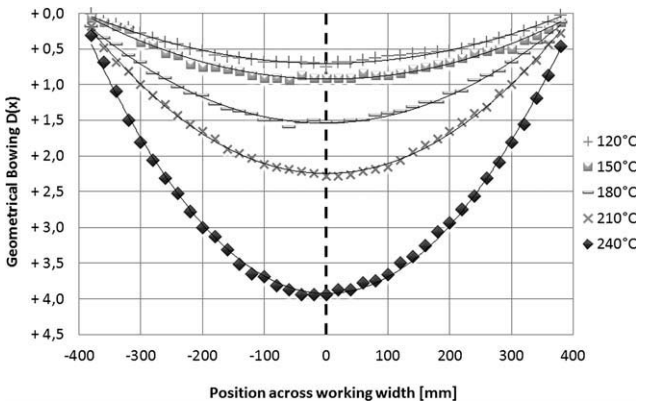

Figure 7. Geometrical bowing $D(x)$ across the working width for films annealed in the TDO at different temperatures.

polarized light. The anisotropy of the biaxially stretched PET film converts the circular polarization of the light that is vertically incident on the film into elliptical polarization. The receiver module detects the azimuthal angle of the polarization ellipse below the film web, from which the position of the principal axes of the index ellipsoid and hence the molecular orientation angle can be derived.

In the event that the retardation of the film at the measurement position is a multiple of half of the relevant wavelength, there is circularly polarized light once again after the film due to the circular polarization of the light beam of the transmitter module. As the evaluation of the azimuthal angle of an approximately circular polarization ellipse leads to ambiguous measurement values, two diode lasers having two different wavelengths ($\lambda_1 = 633$ nm and $\lambda_2 = 650$ nm) were used in the transmitter module as a light source to improve the signal quality. These lasers hit two separate detector surfaces. The two light beams having a diameter of about 10 mm pass through the film in a distance of 50 mm.

If the ellipticity of the polarization ellipse of the beam of wavelength λ_1 that is detected in the receiver module is less than a predefined lower limit, then there is automatic switching to evaluation of the azimuthal angle of the second light source (λ_2). The polarization ellipse of the second light source is then evaluated until its ellipticity is again less than a lower limit and there is then switching back to the measurement signal of the first light source. Due to the small spectral interval between the two wavelengths, dispersion-related changes to the angular position of the azimuthal ellipse can in this case be neglected. The coordinate system for offline measurement from Figure 5 was also used for the inline measurement.

With a traveling film web, 1000 measurements were, respectively, taken with a measurement frequency of 50 Hz for 20 s at the positions −300, −200, −100, 0, +100, +200, and +300 mm after each other and a moving average calculated over 30 measurement points.

RESULTS

Geometrical Bowing

The measured geometrical bowing across the working width can be seen Figure 7. It can be represented by a second order polynomial function (see above).[22] The progressive nature of geometrical bowing with increasing annealing temperature in the TDO (Figure 8) and the ways of reducing geometrical bowing have already been discussed by Yamada.[14]

Shrinkage

The shrinkage measurements are shown in Table I and Figure 9. The curve labeled "annealing temperature (TDO) = 70°C" in Figure 9 indicates the shrinkage values for Film samples 1–5. These film samples were annealed at 70°C in the TDO—i.e., below the glass transition temperature. These samples were subsequently annealed in the shrinking oven at temperatures between 120°C and 240°C.

The curve "annealing temperature (TDO) = free shrinkage temperature" represents the shrinkage of Film samples 6–10. For these samples the shrinkage temperature corresponded to the annealing temperature in the TDO. The relevant temperatures at which the films were annealed in the shrinking oven are plotted on the abscissa.

It can be seen that the curve for the shrinkage values for the Film samples that were annealed at 70°C becomes ever steeper with increasing shrinkage temperature. In contrast, the MD shrinkage values for the films that were annealed between

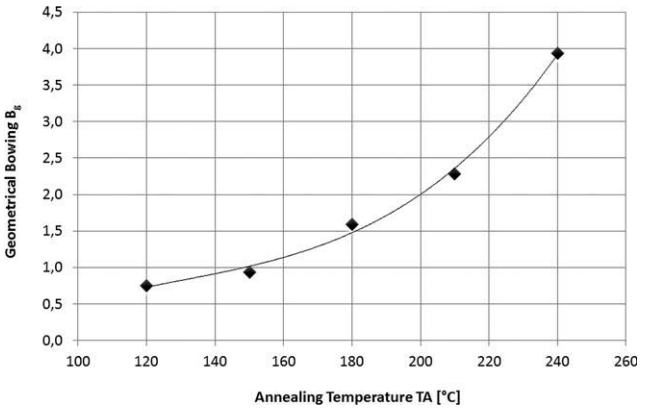

Figure 8. Maximum geometrical bowings B_{max} as a function of the annealing temperature T_A in the TDO.

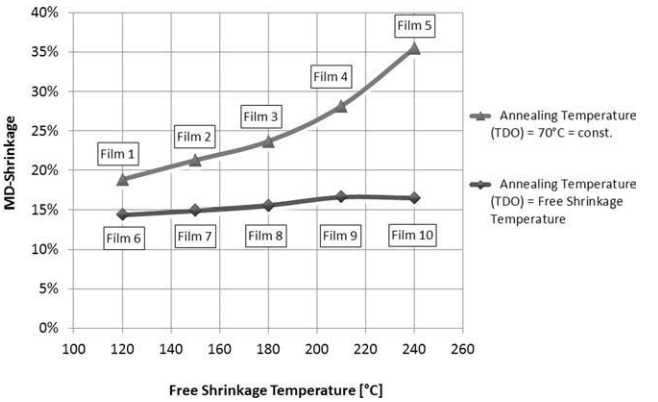

Figure 9. MD shrinkage of Film samples 1–10.

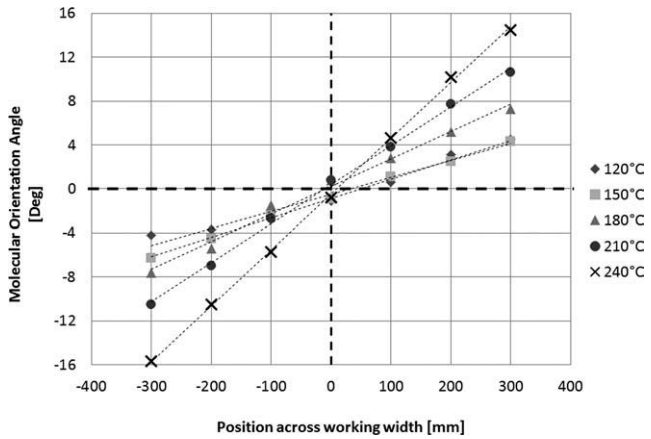

Figure 10. Molecular orientation angle across the working width for films annealed at different temperatures during their manufacture; Position 0 mm corresponds to the center of the working width.

120°C and 240°C and shrunk at the same temperature remain approximately constant across the whole shrinkage temperature range.

The MD shrinkage of the film annealed at 70°C and shrunk at 240°C (Film sample 5) is 35.5%. After annealing in the TDO at 240°C (Film sample 10) this film still shrinks in the MD by about 16.5% on subsequent free annealing in the shrinking oven. Therefore, annealing in the TDO at 240°C reduces the MD shrinkage by 19%.

The difference between the shrinkage values of film samples annealed in the TDO below and beyond the glass transition temperature in Table I and Figure 9 corresponds to the reduction in MD shrinkage during annealing. The reason for the reduction in MD shrinkage is on the one hand the relaxation of orientated amorphous molecular chains in *trans* conformation and subsequent transformation to the *gauche* conformation and on the other hand the growth of the crystalline regions with MD orientation.

Molecular Orientation Angle—Offline Measurement Values

Figure 10 shows the linear profile of the molecular orientation angle across the working width measured offline for the films

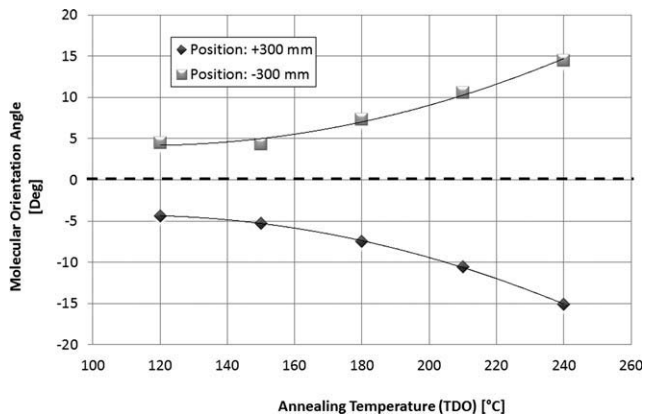

Figure 11. Molecular orientation angle at ±300 mm as a function of the annealing temperature in the TDO.

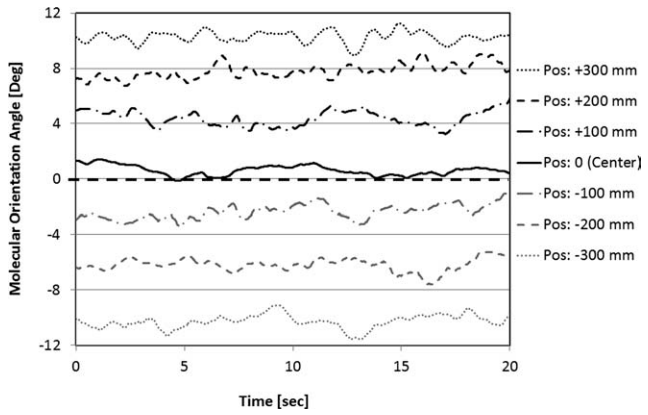

Figure 12. Online measurement of the molecular orientation angle of Film sample 9 (annealing temperature during manufacture: 210°C) at different positions across the working width; Position 0 mm corresponds to the center of the working width; sampling frequency: 50 Hz.

annealed in the TDO at temperatures between 120°C and 240°C (Film samples 6–10). At the center of the working width (position 0 mm) the 0° angle corresponds to an average molecular orientation direction perpendicular to the MD. Analogous to geometrical bowing, the absolute values of the molecular orientation angle at the edges of the film web (at $x = \pm 300$ mm) increase progressively with increasing annealing temperature (Figure 11).

Online Measurement of the Molecular Orientation Angle

The molecular orientation angle across the working width for Film sample 9 (annealed in the TDO at 210°C) is shown in Figure 12. Measurement values were recorded online at seven fixed positions across the working width for 20 s in each case. The minimum, maximum and average values of the molecular orientation angle in the MD at different positions across the working width are displayed in Figure 13. The deviation of the measurement values within the 20-s period was at maximum 2.5° (MD trend at the positions: −300 mm and +100 mm), and the standard deviation was at maximum 0.5°. These deviations can arise due to small temperature or thickness variations during

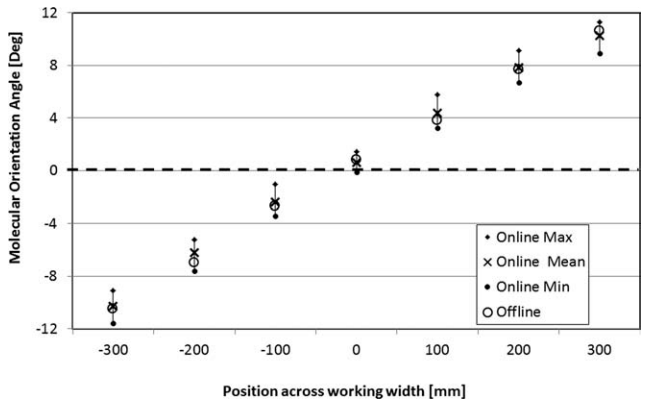

Figure 13. Minimum, maximum and average values for online measurement and offline measurement results of Film sample 9 (annealing temperature in the TDO: 210°C) at different positions across the working width.

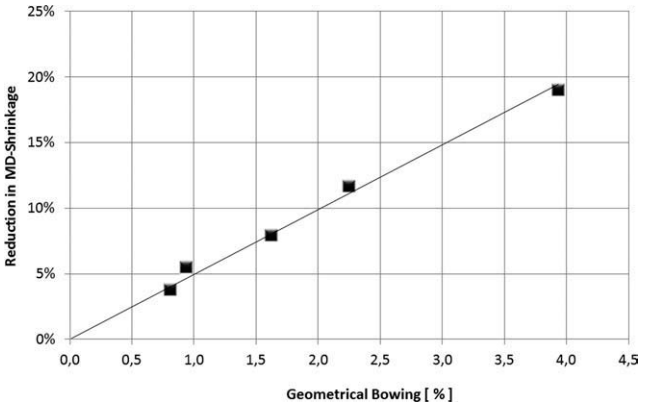

Figure 14. Reduction in the MD shrinkage as a result of annealing in the TDO as a function of the geometrical bowing in sequentially stretched PET films; Measurement position: 0 mm.

the film stretching. In addition, in Figure 13, the values of the molecular orientation angle measured offline in the laboratory using the polarimeter are shown. The maximum deviation between the offline and mean online values was 0.8° at a TD position of −200 mm. All the values of the molecular orientation angle measured in the laboratory lie within the range of the values measured online.

DISCUSSION

Geometrical Bowing and Reduction of MD Shrinkage in the Annealing Zone

There are two main causes for the reduction in shrinkage in the MD as a result of annealing in the TDO.[5–7] First, the shrinkage of the film is reduced due to the relaxation of the *trans* molecules in the amorphous regions at temperatures above the glass transition temperature. The greater the number of molecular chains that switch from *trans* to *gauche* conformation as a result of relaxation, the less the residual shrinkage that remains in the film. Second, the growth of the crystalline regions partially hinders the striving of the amorphous *trans* molecules to relax. With increasing crystalline fraction in the film, there is a consequent increase in the temperature above which the residual shrinkage is observed.

The amount by which the MD shrinkage in the center of the film web is reduced due to these two effects as a result of annealing in the TDO corresponds to the difference between the MD shrinkage in the nonannealed film and the MD shrinkage in the annealed film. This shrinkage difference (see Table I and the difference between the two MD shrinkage curves in Figure 9) is directly proportional to the geometrical bowing (Figure 14).

Thus the amount of MD shrinkage that occurs during the annealing step in the TDO is directly connected to the extent of the geometrical displacement of the film web which results in geometrical bowing. Another indication for this statement is the fact that Film sample 10—which shows a geometrical bowing of almost 4%—shows a minimum in its MD shrinkage across the working width approximately at the center position (Figure 15). Because of the lateral clip forces the relaxation of amorphous *trans* molecules with MD orientation is partially suppressed at the edges of the film web and thus the geometrical displacement of the bowing line decreases toward the edges of the film web. As a result of this the amount of amorphous *trans* molecules with MD orientation in the annealed film web is higher at the edges of the film web compared with the center position, where the maximum displacement of the film web may occur. The higher amount of amorphous *trans* molecules after the annealing step results in a higher MD shrinkage at the edges compared with the center position of the film web.

The reason for the proportionality between the reduction in MD shrinkage and the geometrical bowing (as shown in Figure 14) must be the equilibrium between the shrinkage force and tensile force in the film web in the annealing zone of the TDO. On the one hand the film is pulled against the MD due to the shrinkage force of the relaxing molecular *trans* chains with MD-orientation. The counter force to this is the tensile force in the web which arises due to lateral clip forces, the TD shrinkage force and the tensile force of the roll after passing out of the TDO. At the start of the annealing zone in the TDO there is a high fraction of MD molecular chains in amorphous *trans* conformations, meaning that the MD shrinkage force dominates and there is geometrical bowing. With increasing residence time in the annealing zone of the TDO the amount of MD crystallites increases and the deforming effect of the *trans* molecules is increasingly hindered. In addition, the MD shrinkage force in the film decreases due to the ever lower number of amorphous *trans* chains having MD orientation. Beyond the moment in time when the MD shrinkage force is exactly the same as the web tensile force acting in the MD, the further relaxation of the *trans* chains orientated in the MD and consequent further increase in the geometrical bowing are suppressed.

The relationship between the geometrical bowing and the reduction in MD shrinkage defines the limits for process engineering optimization of key properties of sequentially biaxially stretched films. The minimization of MD shrinkage that can be achieved by selecting an optimum raw material and by optimizing the MD and TD stretching parameters is limited. As in sequential stretching plants there is no opportunity for film relaxation in the MD in the annealing zone, the optimization of the

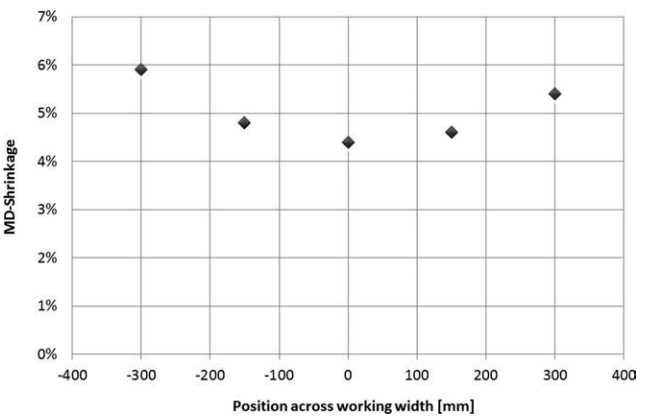

Figure 15. MD shrinkage of Film sample 10 at different positions across the working width (shrinkage temperature 210°C, shrinkage time 30 min).

Table II. Geometrical Bowing B_g in Sequentially Stretched PET Films and the Molecular Orientation Angle (See Also Figure 12)

	Annealing temperature (°C)	Geometrical bowing B_g (-)	Angle of geometrical bowing β_i (°)		Molecular orientation angle α_i (°)	
			$x = -300$ mm	$x = +300$ mm	$x = -300$ mm	$x = +300$ mm
Film sample 6	120	0.75	−1.3	1.3	−4.4	4.5
Film sample 7	150	0.94	−1.6	1.6	−5.3	4.3
Film sample 8	180	1.59	−2.7	2.7	−7.5	7.3
Film sample 9	210	2.28	−3.9	3.9	−10.6	10.6
Film sample 10	240	3.94	−6.7	6.7	−15.1	14.5

MD shrinkage in films that are required to be thermally stable up to 180°C must preferably be carried out using elevated annealing temperatures. The resulting increased geometrical bowing in turn causes inferior property isotropy across the working width. This is why a compromise has to be found in film production processes between optimal shrinkage and minimum bowing.

Geometrical Bowing and Profile of the Molecular Orientation Angle Across the Working Width

Due to the quadratic profile of the geometrical bowing across the working width, the angle β_i between the approximately quadratic geometrical bowing lines and the TD of the film web changes approximately linearly with the molecular orientation angle as a function of the position across the working width. Table II and Figure 16 show the angles β_{-300} and β_{+300} between the TD and the geometrical bowing at the positions ±300 mm and the molecular orientation angle at the same positions. It is clear from Figure 16 that in this series of experiments the molecular orientation angle of the individual films can be converted into the geometrical bowing using a proportionality factor. This hence provides an easy and rapid means for an online measurement system for prediction of the geometrical bowing.

With increasing annealing temperature in the TDO, the molecular orientation angle increases more than the angle β_i enclosed between the approximately quadratic bowing line and the TD.

Despite a process-related inhomogeneity in the film samples, there has to be a similar geometrical bowing and a similar molecular orientation angle at the end of the stretching zone in all samples because the stretching parameters were similar for all sample rolls examined.

The difference in these properties measured in the annealed sample rolls therefore has to arise during the annealing step. More precisely, there has to be a temperature-dependent rotation of the overall molecular orientation angle generated during the annealing step of the sample rolls.

The TD lines drawn on the upper surface of the film web before entering the TDO show a maximum geometrical displacement in the center part of the film web (see Figure 17). Apart from the center part of the film web the TD crystallites will then also adopt a principal orientation direction which is deviating from the TD because of the geometrical displacement of the film web (see lower part of Figure 17). As a consequence of this after the annealing step the principle orientation direction of the TD crystallites will correspond to the TD only at the center part of the film web where the maximum displacement of the geometrical bowing occurs. Because of the quadratic characteristics of the geometrical displacement across the working width, the angle between the main axis of the second crystallite population and the TD of the film web will increase proportionally when approaching the edge parts of the film web.

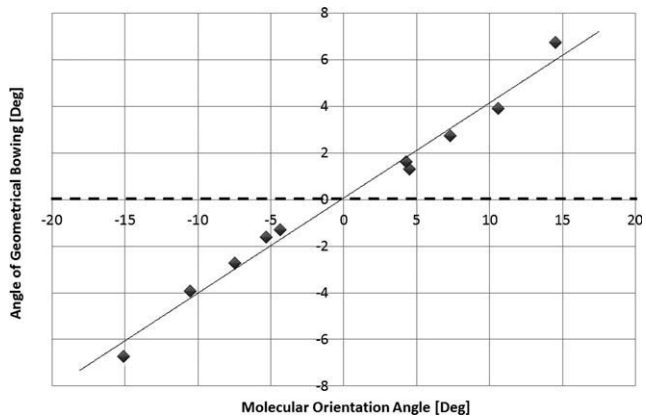

Figure 16. Angle between the geometrical bowing line and the transverse direction of the film web, and molecular orientation angles at the positions −300 mm (negative value) and +300 mm (positive value).

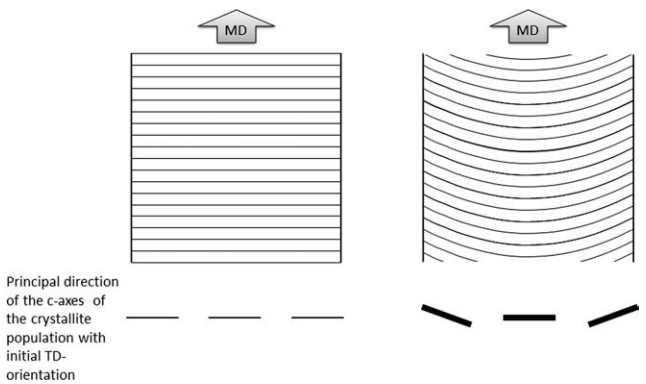

Figure 17. Top view on a rectangular pattern applied to a film web before annealing (left) and after annealing (right); the lower part of the figure shows the effect of the geometrical bowing on the *c*-axis orientation of the TD crystallites.

After the annealing step the principal orientation direction of the TD crystallites includes an angle with the TD of the film web which is at least as big as the angle included by the geometrical bowing and the TD of the film web. Shear stresses or the relaxation of interconnecting tie molecules can lead to a further rotation of crystallites and thus enhance the angle included by the principal orientation direction of the TD crystallites and the TD of the film web. Further information about the actual orientation direction of the crystalline populations along the working width of the film web could be obtained by wide angle X-ray diffraction measurements, which are scheduled in terms of the enhancement of the present experiments.

Because of the relaxation of interconnecting tie molecules, the weaker MD crystallite population could also take up a principal orientation direction differing from the MD beyond the center part of the film web as indicated by X-ray diffraction measurements conducted by MacDonald et al.[18] But independent from the actual orientation direction of the MD crystallite population the molecular orientation angle has to change more intensely along the working width of the film web compared with the direction of the geometrical bowing line or the principal direction of the TD crystallites. The reason for this can be found in the fact that the molecular orientation angle consists of the sum of the principal orientation direction of both of the crystallite populations and also of the principal orientation direction of the amorphous domains. In the absence of the MD crystallite population, the molecular orientation angle might correspond to the angle included by the principal orientation direction of the TD crystallites and the TD of the film web. The presence of the MD crystallites and the *trans* molecules oriented parallel to the MD of the film web adds a MD coordinate to the orientation direction of the TD crystallites. Because of this the molecular orientation angle will exceed the angle between the principal orientation direction of the TD crystallite population or the geometrical bowing line and the TD of the film web. The difference between the overall molecular orientation direction and the *c*-axis orientation of the TD crystallites therefore strongly depends on the development of the MD coordinate of the crystallite populations, e.g., by means of an increase of the MD stretching ratio.

The stronger the MD coordinate is developed compared with the TD coordinate, the more the *c*-axis orientation of the TD crystallites will differ from the overall molecular orientation direction.

Online Measurement of the Molecular Orientation Angle

The good agreement between the offline measurements and the online measurement data shows that online measurements allow reliable and accurate determination of the molecular orientation angle on the moving film web.

Contact-less online measurement of the molecular orientation angle also allows determination of the geometrical bowing during the film production. This means less laboratory work and accelerated process optimization. The extent to which the proportional relationship is dependent on material and process parameters such as the molecular weight, intrinsic viscosity, rate of crystallization, rate of relaxation, and the state of orientation before and after the transverse stretching has to be investigated in further studies.

Online orientation measurement has other potential uses, for example for the manufacture of optical films. Here, the molecular orientation angle is a direct measure of the quality of the film. Besides being of use for the manufacture of protective films for polarizers, it allows direct monitoring of the effects of parameter changes and hence faster and more efficient process optimization. For this the use of the online orientation sensor is not limited to a specific polymer type or raw material.

REFERENCES

1. Heffelfinger C. J. *Polym. Eng. Sci.* **1978,** *18*, 1163.
2. Blumentritt B. F. *J. Appl. Polym. Sci.* **1979,** *23*, 3205.
3. Chang, H.; Schultz, J. M.; Gohil, R. M. *J. Macromol. Sci. B* **1993,** *32*, 99.
4. Gohil, R. M. *J. Appl. Polym. Sci.* **1993,** *48*, 1635.
5. Bhatt, G. M.; Bell, J. P. *J. Polym. Sci.* **1976,** *14*, 575.
6. Mody, R.; Lofgren, E. A.; Jabarin, S. A. *J. Plast. Film Sheet* **2001,** *17*, 152.
7. Heffelfinger, C. J.; Schmidt, P. G. *J. Polym. Sci.* **1965,** *9*, 2661.
8. Pakhomov, P. M.; Shablygin, M. V.; Tsaplin, V. A.; Baranova, S. A.; Vysotskaya, Z. P. *Polym. Sci. U. S.S. R.* **1983,** *25*, 672.
9. Prevorsek, D. C.; Tirpak, G. A.; Harget, P. J.; Reimschuessel, A. C. *J. Macromol. Sci. B* **1974,** *9*, 733.
10. Schmidt, P. G. *J. Polym. Sci. A* **1963,** *1*, 1271.
11. Cakmak, M. In Film Processing; Kanai, T.; Campbell, G. A., Eds.; Hanser: Munich, **1999.**
12. Fischer, E. W.; Fakirov, S. J. *Mater. Sci.* **1976,** *11*, 1041.
13. Yamada, T.; Nonomura, C.; Matsuo, T. *Int. Polym. Process.* **1995,** *10*, 334.
14. Yamada, T.; Nonomura, C. J. *Appl. Polym. Sci.* **1994,** *52*, 1393.
15. Macdonald, W. A.; Mackerron, D. H.; Brooks, D. W. In pet Packaging Technology; Brooks, D. W.; Giles, G. A., Eds.; CRC Press: Boca Raton, **2002;** p 128.
16. Yamada, T.; Nonomura, C. J. *Appl. Polym. Sci.* **1993,** *48*, 1399.
17. Jungnickel, B. J. *Makromol. Chem.* **1984,** *125*, 121.
18. Macdonald, W. A.; Mackerron, D. H.; Brooks, D. W. In pet Packaging Technology; Brooks, D. W.; Giles, G. A., Eds.; CRC Press: Boca Raton, **2002;** p 130, Figure 5.10.
19. Kim, G. H.; Kang, C.-K.; Chang, C. G.; Ihm, D. W. *Eur. Polym. J.* **1997,** *33*, 1633.
20. Boger, S. Online-Bestimmung der Orientierung in den nichtkristallinen Bereichen von Polymerfasern mittels der Methode der polarisierten Fluoreszenz. Ph.D. Thesis, University of Stuttgart, **2002.**
21. Chipman, R. A. In Handbook of Optics, 2nd ed.; Bass, M., Ed.; McGraw-Hill: New York, **1995;** Vol. *II*, p. 22.1f.
22. Koerber, A. *German Patent Application No. 10 20 10 011 864,* **2010.**